

Higgs Boson Production in $\gamma\text{-}\gamma$ Collision in TeV Region^{*}

Ryuichi NAJIMA

Faculty of General Education, Yokohama College of Commerce, Yokohama 230

ABSTRACT

We investigate the possibilities of Higgs boson detection in $\gamma\text{-}\gamma$ collision using e^+e^- linear colliders which are now being extensively studied at several laboratories. The cross sections of Higgs boson production and main background process are calculated and it is suggested that the reaction $\gamma\gamma \rightarrow H \rightarrow ZZ$ is very effective to search heavy Higgs boson in almost all the mass range from $2M_Z$ to 1 TeV.

^{*} Work supported in part by the Research Institute of Yokohama College of Commerce

The Glashow-Weinberg-Salam theory [1] of electroweak interaction (we call electroweak theory hereafter) succeeds to describe low energy phenomena and the properties of W and Z bosons. But two important entries of the theory have not been yet discovered, i.e, Higgs boson and top quark. Especially the former is indispensable to the renormalizability [2] and the unitarity [3] of the theory and further its property will offer important information for the beyond the standard theories.

In the experiment of LEP200, it is known that we can well look for the Higgs bosons of the mass below 100GeV. If the mass is heavier than this, we must leave the search to the next TeV-colliders of two different approaches, that is, $pp(p\bar{p})$ colliders like SSC and LHC or e^+e^- linear colliders which are now planned at several laboratories. These two ways have complementary aspects, but as far as the Higgs boson search is concerned, e^+e^- linear colliders have many advantages owing to much less background events.

It has been known, however, that in the e^+e^- linear colliders the bremsstrahlung from the high density beam-beam pulse interaction (beamstrahlung hereafter) induces large and fractional energy loss to both the electron and positron bunches and becomes very serious matter in the TeV-energy collision. The $\gamma\text{-}\gamma$ collision is considered to be an alternative to compensate this difficulty and the technological feasibility about the photon beams are now being studied extensively [4]. Here we discuss the physics aspects of $\gamma\text{-}\gamma$ collision mainly concentrating on Higgs boson production and its detection.

In $\gamma\text{-}\gamma$ collision Higgs boson is produced through the 1-loop diagram which contains W -boson and fermions (Fig. 1). It is the inverse process of Higgs boson decaying into two photons which was first calculated by Vainshtein et al. [5]. In the following we calculate the cross sections of processes (a) $\gamma\gamma \rightarrow H \rightarrow W^+W^-$ (heavy Higgs case), (b) $\gamma\gamma \rightarrow H \rightarrow b\bar{b}$ (intermediate Higgs case) and their background reactions.

$$(a) \gamma\gamma \rightarrow H \rightarrow W^+W^-$$

This process is shown in Figure 2 where the $\gamma\gamma H$ blob denotes the same diagram as

Figure 1 and we hereafter consider only the contribution of the top quark in the fermion loop.

The amplitude is given as

$$T = \varepsilon_\alpha \varepsilon_\beta A_{\alpha\beta} \frac{1}{s - M_H^2 + iM_H \Gamma_H} B_{\mu\nu} \varepsilon_\mu \varepsilon_\nu, \quad (1)$$

where ε_α and ε_β are the incident photon polarization vector, ε_μ and ε_ν are those of the outgoing W^- and W^+ respectively. $A_{\alpha\beta}$ and $B_{\mu\nu}$ denote $\gamma\gamma H$ blob and W^+W^-H vertex. For the total decay width of the Higgs boson Γ_H , we include the decay modes $H \rightarrow \tau^+\tau^-$, $c\bar{c}$, $b\bar{b}$, $t\bar{t}$, W^+W^- , ZZ depending on various M_H and m_t . In Figure 3 the solid curve corresponds to Γ_H for $m_t = 100\text{GeV}$, and the dashed line to $M_H/10$, the dot-dashed line to $M_H/20$ and the dotted line to $M_H/50$, these line also represents $E_{beam}/5$, $E_{beam}/10$ and $E_{beam}/25$ respectively (Beam energy width should be narrower than Γ_H for the signature to overcome the background). From the equation (1), we immediately get the spherical distribution

$$\frac{d\sigma}{d\Omega} = \frac{\Gamma_{H \rightarrow \gamma\gamma} \Gamma_{H \rightarrow W^+W^-}}{(s - M_H^2)^2 + \Gamma_H^2 M_H^2}, \quad (2)$$

and $\sigma(s) = 4\pi d\sigma/d\Omega$. In the following we consider the signature of Higgs boson only for the values of σ and $d\sigma/d\Omega$ on the pole. In Figure 4 we will give the total cross sections for both reactions $\gamma\gamma \rightarrow H \rightarrow W^+W^-$ and the background $\gamma\gamma \rightarrow W^+W^-$ [6] [7]. The latter reaction contains three diagrams in unitary gauge (Figure 5) and its angular distributions for various \sqrt{s} are shown in Figure 6. In Figure 4 the behavior of σ corresponding to the Higgs boson production depends mainly on the cancellation of top quark and W -boson loop in $\gamma\gamma H$ blob and we see that the total cross section for the reaction $\gamma\gamma \rightarrow H \rightarrow W^+W^-$ are one order less than that of $\gamma\gamma \rightarrow W^+W^-$ around 250GeV . However the angular distribution shown in Figure 7 indicates that the effects of the Higgs boson production can still be seen if we use the cut condition $|\cos\theta_{CM}| < 0.35$.

If the mass of Higgs boson is larger than 300GeV, we should consider the polarization of W -boson* or the process $\gamma\gamma \rightarrow H \rightarrow ZZ$ (the background reaction $\gamma\gamma \rightarrow ZZ$ does not occur in the tree level).

Figure 8 shows that a very peculiar feature happens when M_H equals to 700GeV with $M_T = 200GeV$. This is because that both the real and imaginary parts of $\gamma\gamma H$ vertex vanish at the same time(i.e, the decay mode $H \rightarrow \gamma\gamma$ is forbidden) by the perfect cancellation between top quark and W -boson loops. These situation convinces us that $\gamma\text{-}\gamma$ collision can be a very interesting tool to look into the heavy particles world taking various contributions of the loop diagrams into consideration even after both top quark and Higgs boson are discovered.

(b) $\gamma\gamma \rightarrow H \rightarrow b\bar{b}$

Figure 9 shows the differential cross section for intermediate Higgs boson production ($M_H = 140GeV$) through the process $\gamma\gamma \rightarrow H \rightarrow b\bar{b}$. It is found that we can get enough $b\bar{b}$ pairs from Higgs decay(flat lines) compared with the background $\gamma\gamma \rightarrow b\bar{b}$ (solid curve). However, since the total decay width of Higgs boson is very small(0.7 MeV), it seems to be rather difficult to make the energy width of photon beam narrower than Γ_H (need for very severe monocromatization [9])

We have calculated the cross section of the heavy and intermediate Higgs boson production and compared with main background process. It has been shown that Higgs boson in the mass range $200GeV < M_H < 300GeV$ can be detected using the decay mode $H \rightarrow W^+W^-$ only(but we need the narrow beam energy width less than $E_{beam}/20$). If M_H is larger than 300GeV, we should consider the polarization of W -boson or the decay mode $H \rightarrow ZZ$, and further, for the case $M_H > 600GeV$, we may take longitudinally polarized Z -boson to detect the signature of Higgs boson(the ratio of decay width $H \rightarrow$

* W -bosons from Higgs decay are almost longitudinally polarized, but in the background reaction $\gamma\gamma \rightarrow W^+W^-$, the ratio of W_L to W_T is about $1/10(\sqrt{s} = 400GeV)$ [8] .

ZZ to $H \rightarrow W^+W^-$ is $1/2$). Therefore I would like to emphasize the importance of the calculation to the process $\gamma\gamma \rightarrow ZZ$ for further study of $\gamma\text{-}\gamma$ collision. Finally it should be noted that as the reaction we considered here is "single" Higgs production, the particle identification is very easy and clear compared with $pp(p\bar{p})$ or e^+e^- collisions.

I would like to thank Y.Shimizu for valuable discussion and suggestions throughout this work. I am also grateful to H.Tanaka, J.Fujimoto and the other members of the theoretical group of TRISTAN. Discussions about beamstrahlung and technological aspects of $\gamma\text{-}\gamma$ collision with S.Kawabata, I.Endo, T.Tauchi and H.Yokoya was very useful. The numerical calculation was performed at the Computer Center of KEK.

REFERENCES

1. S. L. Glashow, *Nucl. Phys.* **B22**, 579 (1961);
S. Weinberg, *Phys. Rev. Lett.* **19**, 1264 (1967);
A. Salam, in *Elementary Particle Theory*, edited by N. Svartholm (Almqvist and Wiksell, Stockholm, 1969), P.367.
2. G. 't Hooft, *Nucl. Phys.* **B33**, 173 (1971).
3. B. W. Lee, C. Quigg and H. B. Thacker, *Phys. Rev. Lett.* **38**, 883 (1977).
4. I. F. Ginzburg et al., *Nucl. Instr. Meth.* **205**47(1983);
R. Blankenbecler and S. D. Drell, *Phys. Rev. Lett.* **61**, 15 (1988); erratum-ibid.
62: 116(1989).
5. A. I. Vainshtein et al., *Sov. J. Phys.* **30**, 711 (1979).
6. I. F. Ginzburg et al., *Nucl. Phys.* **B228**, 285 (1983).

7. M. Katuya, *Phys. Lett.* **124**, 421 (1983).
8. H. Tanaka, private communication.
9. I. F. Ginzburg et al., *Nucl. Instr. Meth.* **2195**(1983) .

FIGURE CAPTIONS

- 1) Lowest order Feynman diagrams for $\gamma\gamma \rightarrow H$ in unitary gauge: fermion loop (a) and W -boson loop(b,c).
- 2) Feynman diagrams for $\gamma\gamma \rightarrow H \rightarrow W^+W^-$. $\gamma\gamma H$ blob denotes the same diagram as Figure 1.
- 3) Decay width of Higgs boson for $m_t = 100\text{GeV}$ (solid curve) compared with $M_H/10$ (dashed line), $M_H/20$ (dot-dashed line) and $M_H/50$ (dotted line).
- 4) Total cross sections for $\gamma\gamma \rightarrow W^+W^-$ (solid curve) and $\gamma\gamma \rightarrow H \rightarrow W^+W^-$ (on pole of Higgs boson) for (a) $m_t=30\text{GeV}$, (b) $m_t=60\text{GeV}$, (c) $m_t=100\text{GeV}$ and (d) $m_t=200\text{GeV}$.
- 5) Lowest order Feynman diagrams for $\gamma\gamma \rightarrow W^+W^-$.
- 6) Angular distributions for $\gamma\gamma \rightarrow W^+W^-$: (a) $\sqrt{s}=200\text{GeV}$, (b) $\sqrt{s}=400\text{GeV}$, (c) $\sqrt{s}=600\text{GeV}$, (d) $\sqrt{s}=800\text{GeV}$ and (e) $\sqrt{s}=1\text{TeV}$.
- 7) Angular distributions($\sqrt{s} = 400\text{GeV}$) for $\gamma\gamma \rightarrow W^+W^-$ (solid curve) and $\gamma\gamma \rightarrow H \rightarrow W^+W^-$ (on pole of Higgs boson) for various m_t : $m_t=60\text{GeV}$ (dotdash), $m_t=90\text{GeV}$ (dots) and $m_t=150\text{GeV}$ (dashes).
- 8) Total cross sections for $\gamma\gamma \rightarrow W^+W^-$ (solid line) and $\gamma\gamma \rightarrow H \rightarrow W^+W^-$ (on pole of Higgs boson) for various m_t : $m_t=90\text{GeV}$ (dott-dashed curve), $m_t=150\text{GeV}$ (dotted curve), $m_t=200\text{GeV}$ (solid curve) and $m_t=250\text{GeV}$ (dashed curve).

9) Angular distributions for $\gamma\gamma \rightarrow b\bar{b}$ (solid curve) and $\gamma\gamma \rightarrow H \rightarrow b\bar{b}$ (on pole of Higgs boson) for various m_t : $m_t=60\text{GeV}$ (dotdash), $m_t=90\text{GeV}$ (dots) and $m_t=150\text{GeV}$ (dashes).

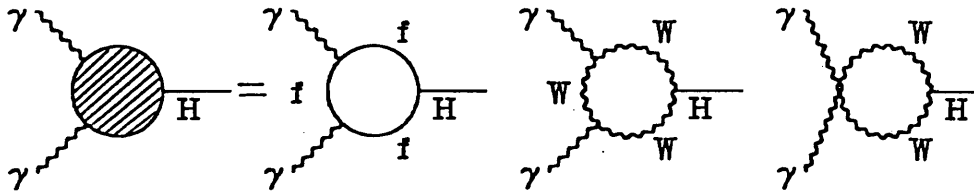


Fig. 1

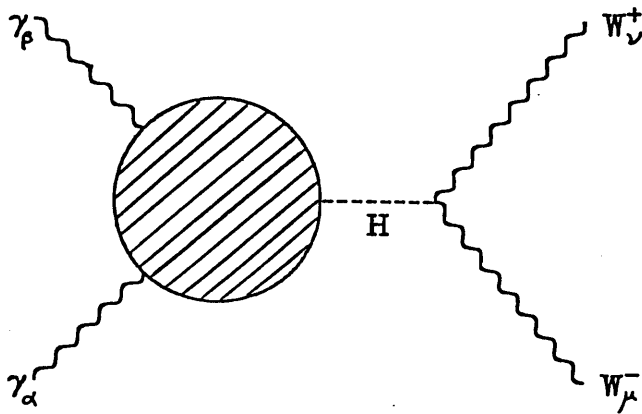


Fig. 2

DECAY WIDTH OF HIGGS BOSON

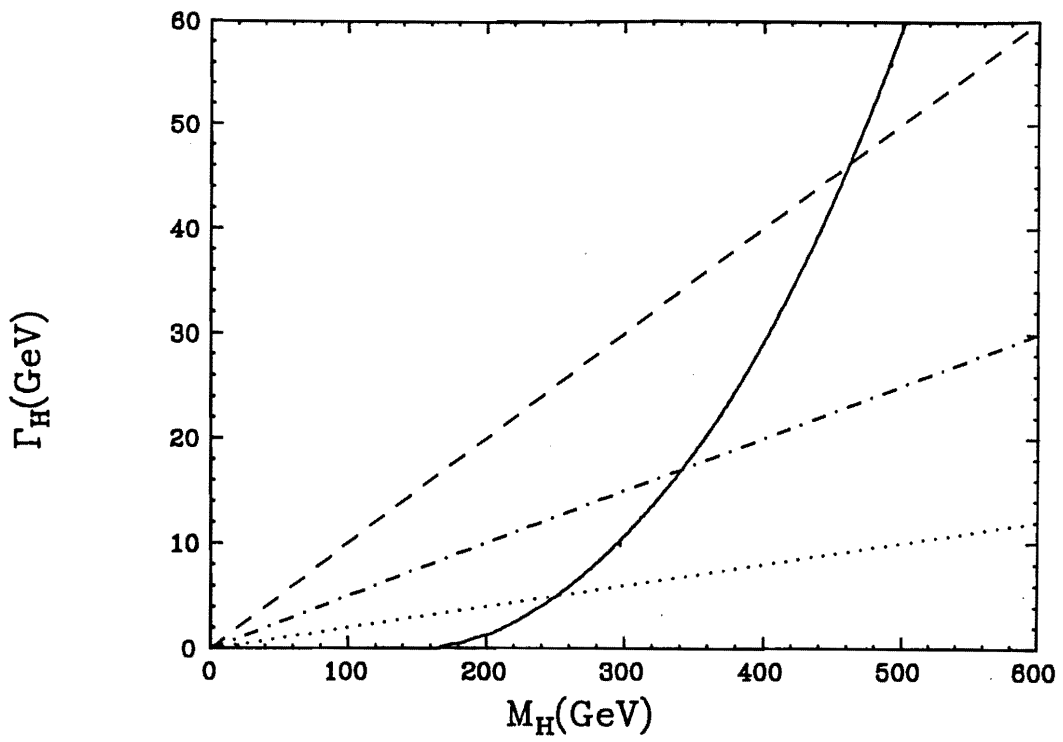


Fig. 3

$\gamma\gamma \rightarrow H \rightarrow W^+W^-$ vs. $\gamma\gamma \rightarrow W^+W^-$

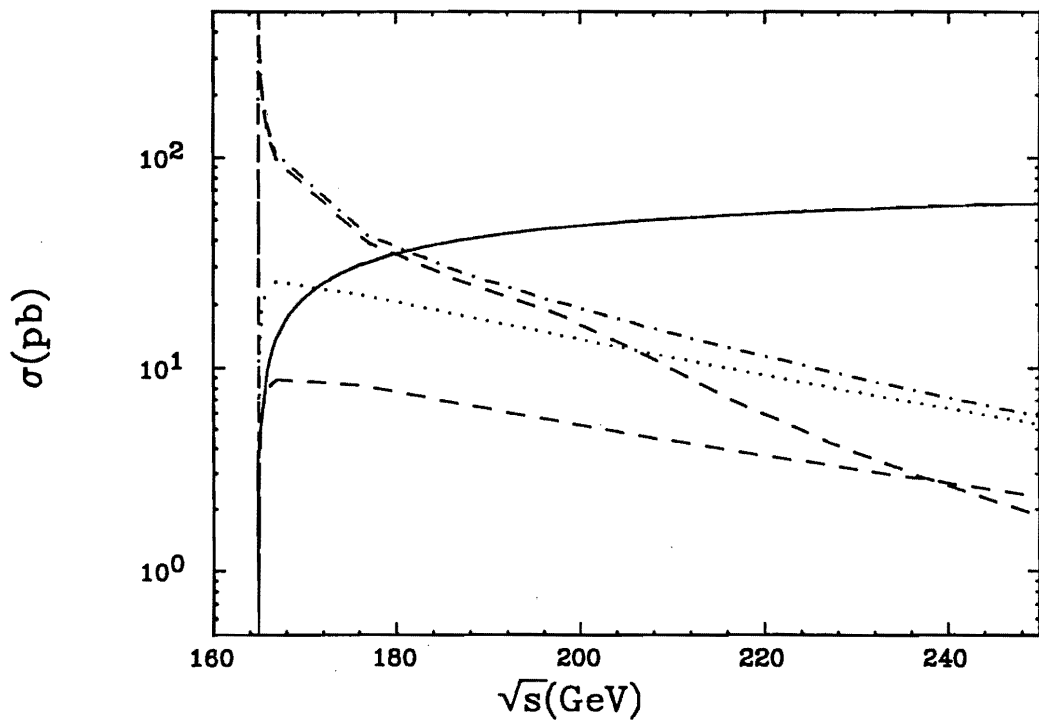


Fig. 4

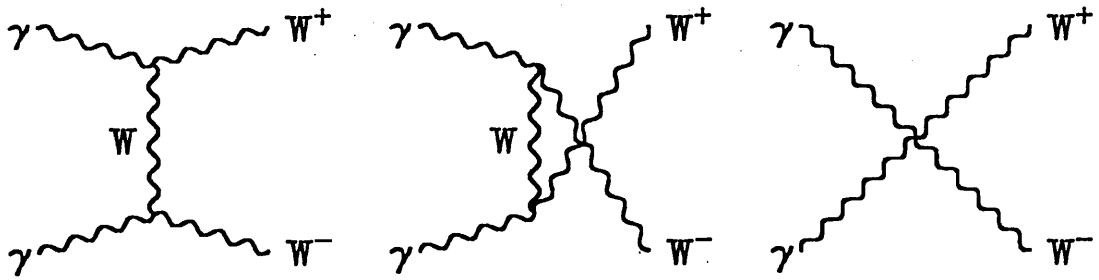


Fig. 5

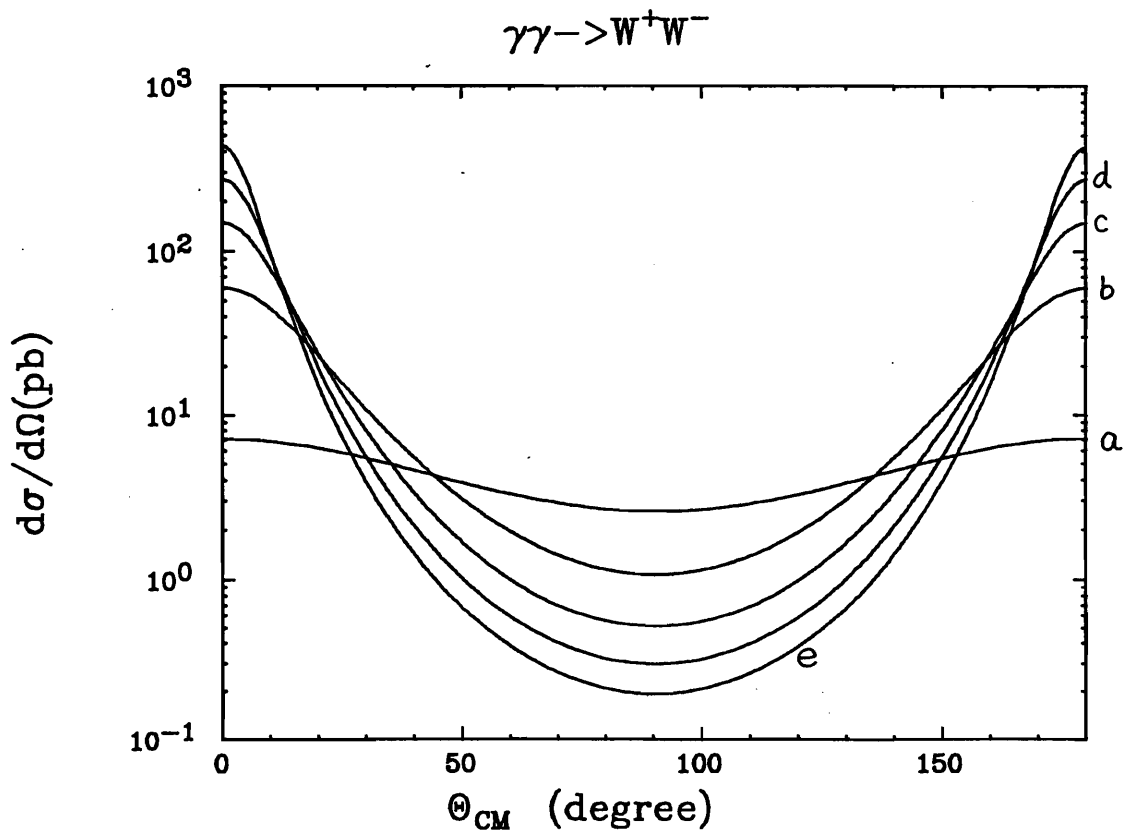


Fig. 6

$\gamma\gamma \rightarrow H \rightarrow W^+W^-$ vs. $\gamma\gamma \rightarrow W^+W^-$

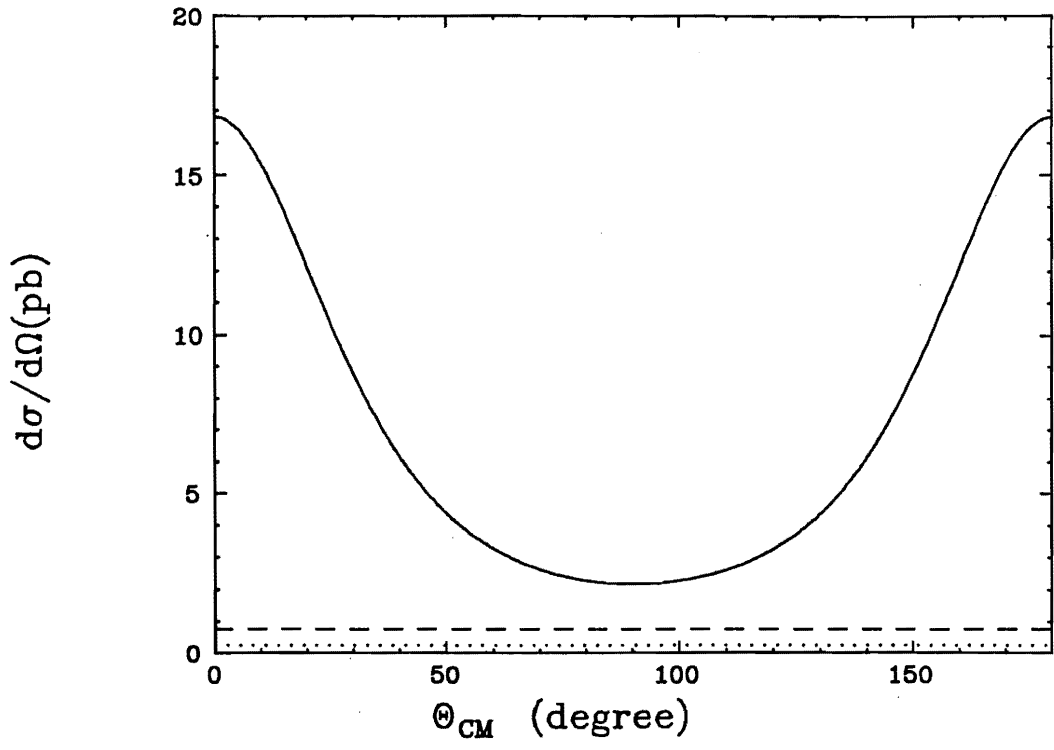


Fig. 7

$\gamma\gamma \rightarrow H \rightarrow W^+W^-$ vs. $\gamma\gamma \rightarrow W^+W^-$

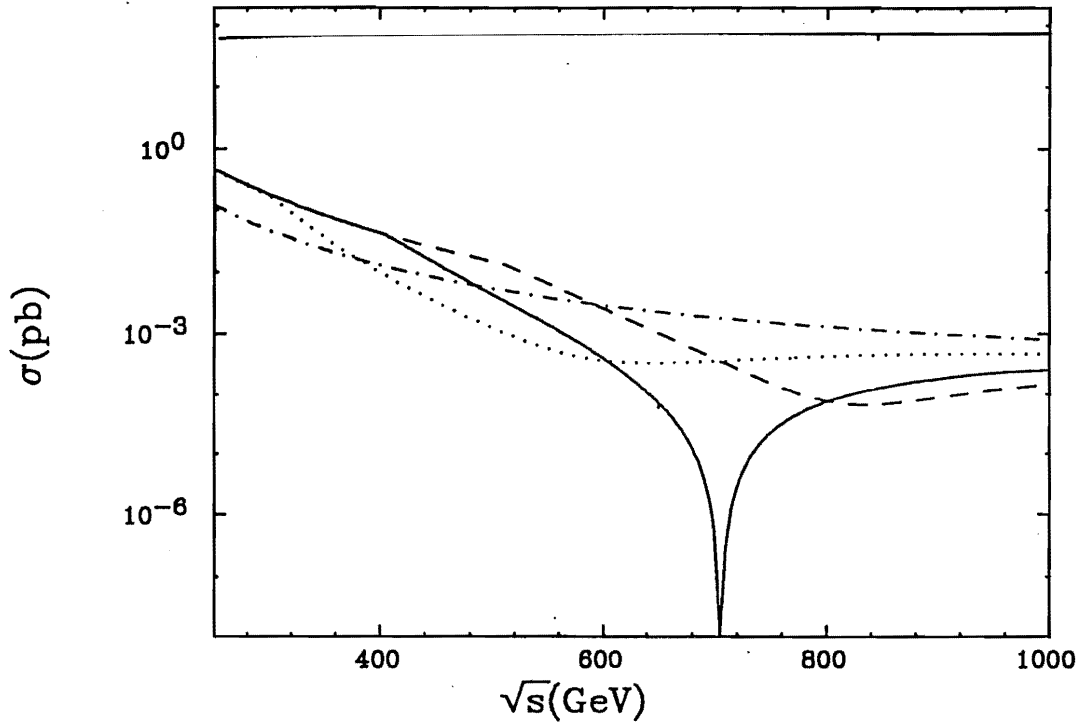


Fig. 8

$\gamma\gamma \rightarrow b\bar{b}$ ($\sqrt{s} = 140\text{GeV}$)

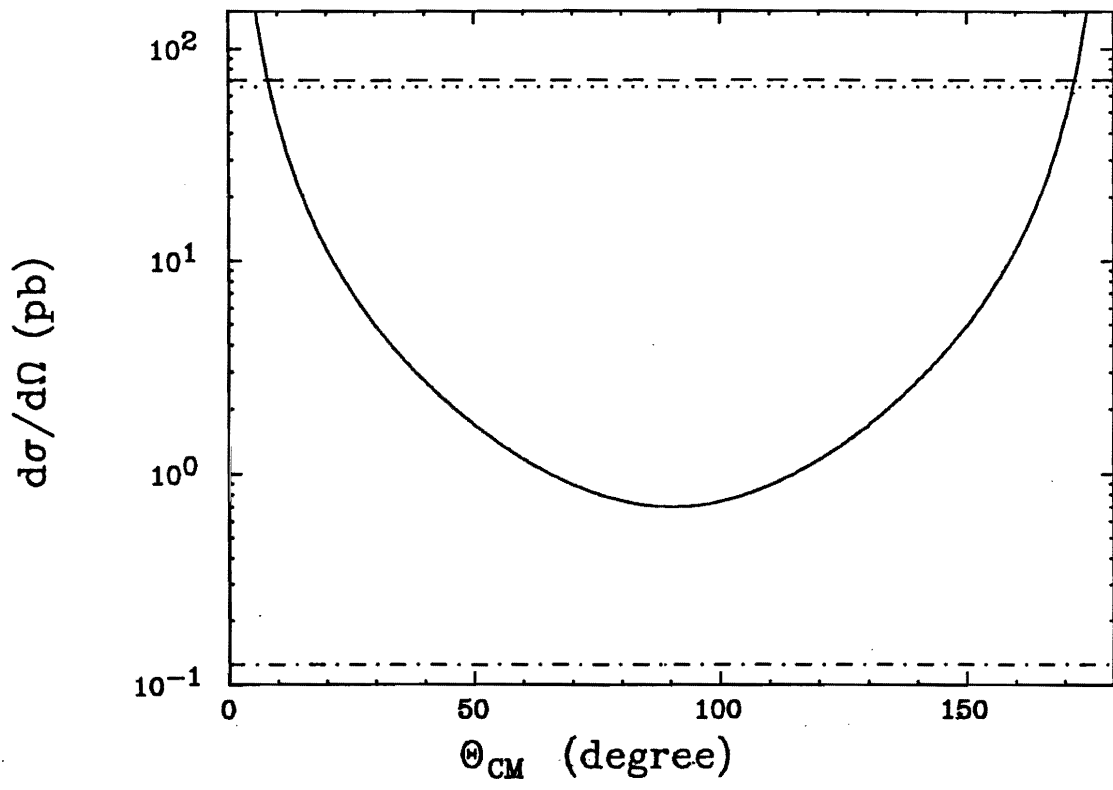


Fig. 9